Received: 2 June 2020 | Revised: 10 July 2020 | Accepted: 12 July 2020

DOI: 10.1002/asl.1005

RESEARCH ARTICLE

Atmospheric Science Letters RMetS

Predictability of European winter 2019/20: Indian Ocean dipole impacts on the NAO

Steven C. Hardiman[1] | **Nick J. Dunstone**[1] | **Adam A. Scaife**[1,2] | **Doug M. Smith**[1] | **Jeff R. Knight**[1] | **Paul Davies**[1] | **Martin Claus**[3,4] | **Richard J. Greatbatch**[3,4]

[1]Met Office, Exeter, UK

[2]College of Engineering, Mathematics, and Physical Sciences, University of Exeter, Exeter, UK

[3]GEOMAR Helmholtz Centre for Ocean Research Kiel, Kiel, Germany

[4]Faculty of Mathematics and Natural Sciences, Kiel University, Kiel, Germany

Correspondence
Steven C. Hardiman, Met Office, FitzRoy Road, Exeter, Devon EX1 3PB, UK.
Email: steven.hardiman@metoffice.gov.uk

Funding information
Met Office Hadley Centre Climate Programme funded by BEIS and Defra

Abstract

Northern Europe and the UK experienced an exceptionally warm and wet winter in 2019/20, driven by an anomalously positive North Atlantic Oscillation (NAO). This positive NAO was well forecast by several seasonal forecast systems, suggesting that this winter the NAO was highly predictable at seasonal lead times. A very strong positive Indian Ocean dipole (IOD) event was also observed at the start of winter. Here we use composite analysis and model experiments, to show that the IOD was a key driver of the observed positive NAO. Using model experiments that perturb the Indian Ocean initial conditions, two teleconnection pathways of the IOD to the north Atlantic emerge: a tropospheric teleconnection pathway via a Rossby wave train travelling from the Indian Ocean over the Pacific and Atlantic, and a stratospheric teleconnection pathway via the Aleutian region and the stratospheric polar vortex. These pathways are similar to those for the El Niño Southern Oscillation link to the north Atlantic which are already well documented. The anomalies in the north Atlantic jet stream location and strength, and the associated precipitation anomalies over the UK and northern Europe, as simulated by the model IOD experiments, show remarkable agreement with those forecast and observed.

KEYWORDS

European winter, Indian Ocean dipole, North Atlantic oscillation, seasonal forecasting, teleconnections

1 | INTRODUCTION

The winter of 2019/20 saw a positive North Atlantic Oscillation (NAO; Figure 1a). This strengthened the north Atlantic storm track, and moved it further poleward, leading to a warm and wet winter in the UK and northern Europe. Indeed, Europe as a whole experienced its warmest winter on record, and February 2020 was the wettest UK February on record. Tropical rainfall can drive the extratropics in winter and affects the NAO (Scaife *et al*., 2017a). In particular, a strong La Niña event can cause a strongly positive NAO (through the

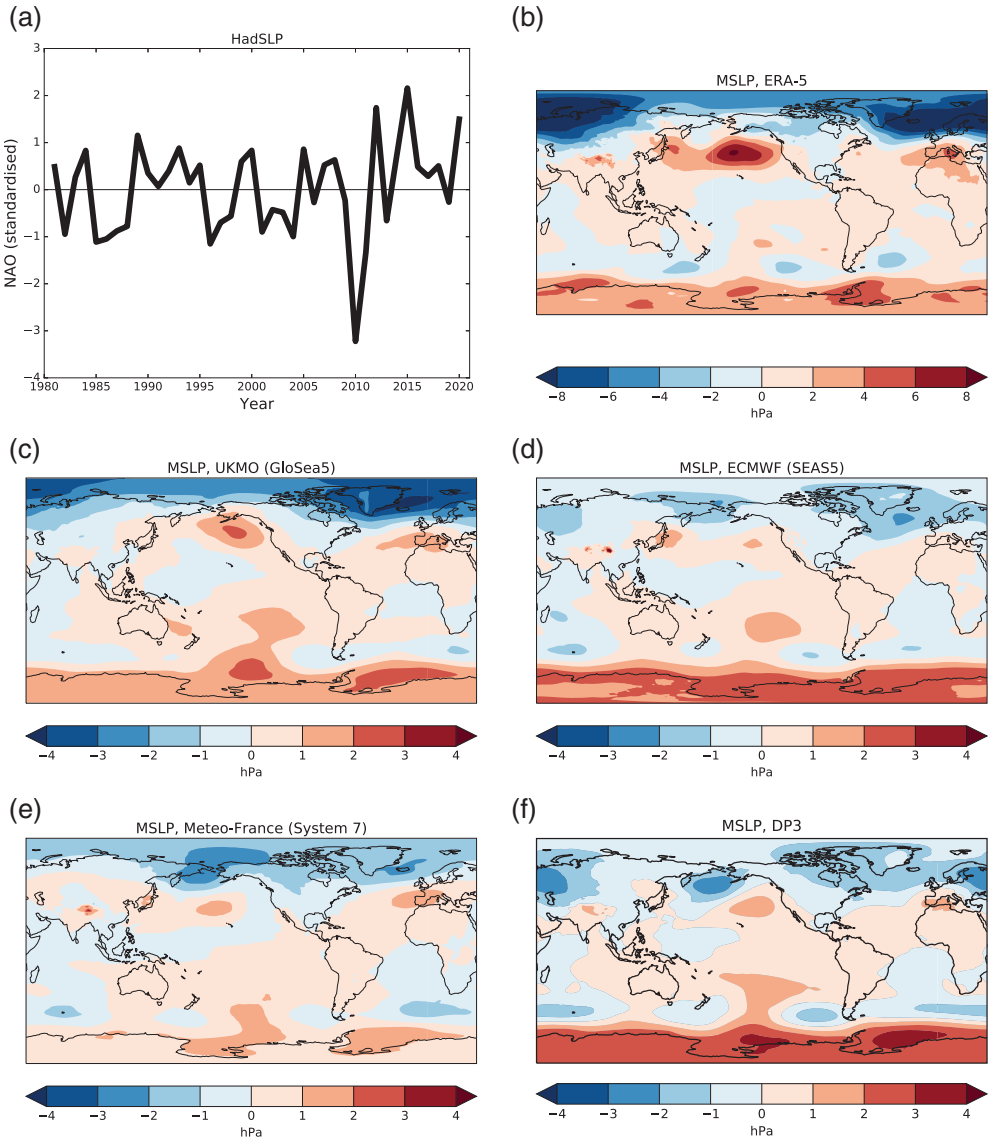

FIGURE 1 Common +NAO signal in models. (a) Standardised North Atlantic Oscillation (NAO) index, HadSLP. Mean sea level pressure (MSLP) anomalies for DJF 2019/20 in (b) the ERA-5 reanalysis, and November 2019 forecasts of MSLP(hPa), for DJF 2019/20, as simulated by the (c) UKMO (GloSea5), (d) ECMWF (SEAS5), and (e) Météo-France (System 7) C3S systems, and the (f) DP3 decadal prediction system. Anomalies in panels (b)–(f) are relative to the respective modelled and observed climatologies formed over the (hindcast) period 1993/4–2016/7. Note the different colour bars for (b) and (c)–(f) – this is consistent with the signal-to-noise paradox (Scaife and Smith, 2018)

teleconnection pathways described in: Ineson and Scaife, 2009; Jiménez-Esteve and Domeisen, 2018; Hardiman *et al*., 2019). However, during this winter, the El Niño Southern Oscillation (ENSO) was in a neutral state.

In winter 2019/20, the observed sea surface temperatures in the west/east parts of the Indian Ocean basin were anomalously warm/cold, leading to a positive Indian Ocean Dipole (IOD; Saji *et al*., 1999; Webster *et al*., 1999) that was the second strongest recorded since 1972 (Doi *et al*., 2020). This paper considers whether it is likely that the positive IOD contributed to the observed positive NAO. The IOD is a coupled atmosphere–ocean phenomenon (Rao *et al*., 2002), with associated planetary wave activity (Min *et al*., 2008; Weller and Cai, 2013), that is known to impact temperatures and rainfall across the globe (Saji and Yamagata, 2003). Furthermore, several seasonal forecasting systems (described in Section 2) captured this strongly anomalously positive IOD in early winter, as well as predicting a positive NAO. A particular focus of the current literature on IOD impacts is Australia (Cai *et al*., 2011; Weller and Cai, 2013) and the southern high latitudes (Liu *et al*., 2007). Nevertheless, a link between Indian Ocean rainfall and the NAO has been previously identified (Hoerling *et al*., 2004; Bader and Latif, 2005; Dahlke, 2015; Gollan and Greatbatch, 2017), teleconnections between the Indian Ocean and the north Atlantic were considered by Fletcher and Cassou (2015), and the NAO was found to be sensitive to Indian Ocean SSTs in the atmosphere only experiments of Baker *et al*. (2019). These studies all use model experiments to demonstrate the link between the Indian Ocean and the NAO. In the present study, we look further into the mechanisms whereby the IOD can influence the north Atlantic using a combination of reanalysis data (see Figure 2) and model experiments. ENSO is

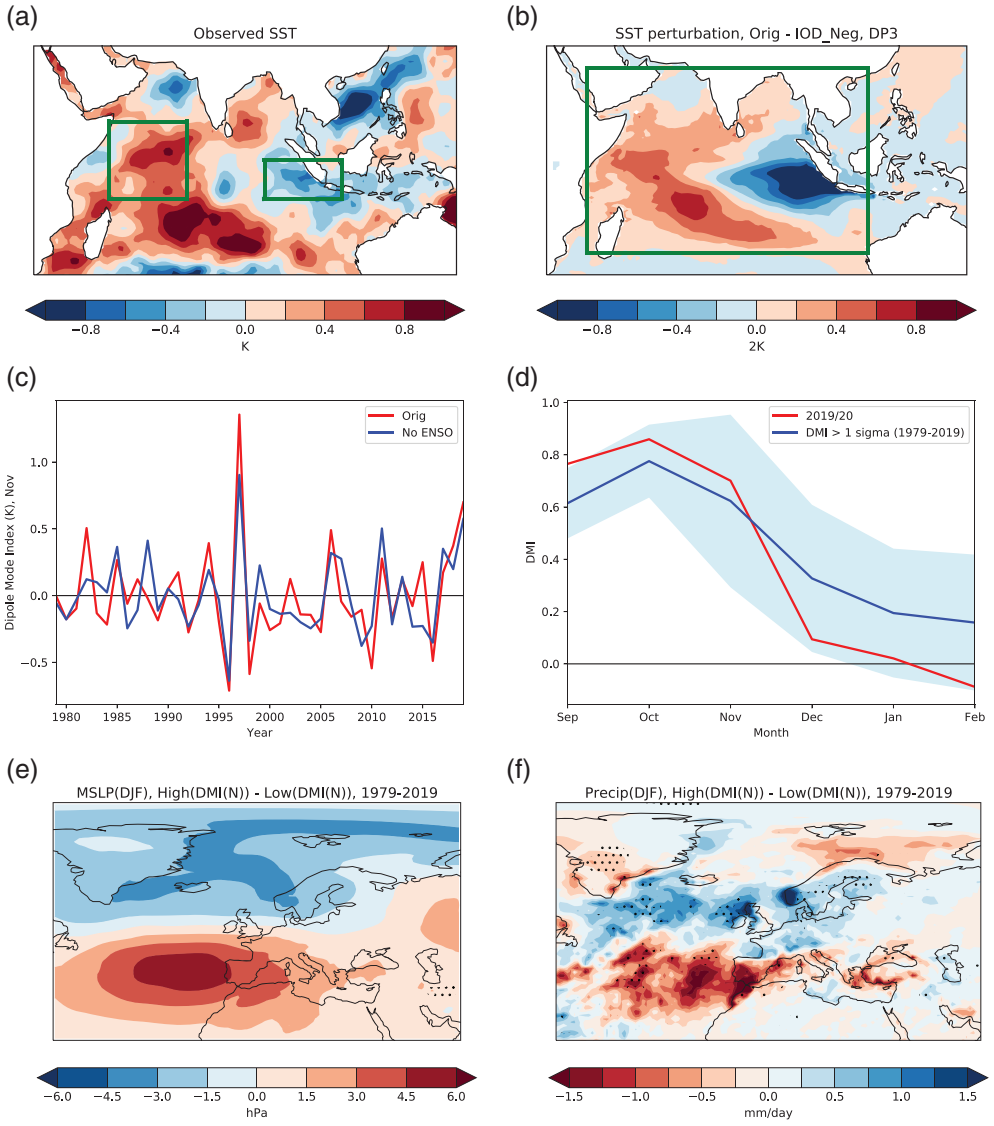

FIGURE 2 Strong positive IOD. (a) Observed SST anomalies (2019–[2014–2018]) for November (HadISST). Green boxes show regions used to define the Dipole Mode Index (DMI = area averaged SST in left box minus right box). (b) SST perturbation, 'Original – IOD_Neg', for November in the IOD experiment. Green box shows the region where the SST was perturbed. Note the colour bar for (b) uses double the values for (a) since (b) shows positive 2019 anomalies minus negative 2019 anomalies. (c) Observed (HadISST) November raw DMI index (red), and with ENSO signal removed using linear regression (blue). (d) Observed DMI evolution during winter 2019/20 (red line) and averaged over all winters with strong positive DMI – where November DMI is greater than plus one standard deviation (blue line, with shading showing the 95% confidence interval). Composite patterns for the IOD [DMI > 1σ – DMI < -1σ, where σ = standard deviation] over the last 40 years (1979/80–2018/19) on (e) MSLP (hPa) and (f) Precipitation (mm/day) are shown, with ENSO signal removed and stippling denoting statistical significance at the 90% level

known to impact the IOD (Marchant *et al.*, 2007; Liu *et al.*, 2014), so the effects of ENSO are removed as far as is possible from our reanalysis composites by using linear regression. We consider how the influence of the IOD on the NAO may have increased the performance of winter forecasts (following on from studies of forecast system performance in earlier winters: Scaife *et al.*, 2017b, Dunstone *et al.*, 2018). This may be particularly important for seasonal forecasting of European winters in the future, since the frequency and intensity of positive IOD events has been observed to increase throughout the twentieth century and is likely to continue to do so due to climate change (Abram *et al.*, 2020).

Section 2 describes the datasets and seasonal forecasting systems used in this study, results of analyses and model perturbation experiments are presented in Section 3, and conclusions are given in Section 4.

2 | DATASETS, SEASONAL FORECAST SYSTEMS, AND EXPERIMENTS

Sea surface temperature (SST) from the Hadley Centre sea Ice and Sea Surface Temperature data set (HadISST; Rayner *et al*., 2003) is used to define the IOD Dipole Mode Index (DMI = SST[50–70°E, 10°S–10°N] – SST [90–110°E, 10°S-Equator]; Saji *et al*., 1999). Mean Sea level pressure (MSLP) from the variance adjusted HadSLP2r dataset, a near real-time update of the Hadley Centre Sea Level Pressure dataset (HadSLP2; Allan and Ansell, 2006) is used to form the NAO index (Figure 1a; NAO index = MSLP[28.5–20°W, 36–40°N] – MSLP [25–16.5°W, 63.5–70°N]; Dunstone *et al*., 2016). All other 'observations' are from the ERA-5 reanalysis dataset (Copernicus Climate Change Service, 2017).

Winter 2019/20 forecasts from the original three C3S (Copernicus Climate Change Service, 2017) seasonal forecast systems are analysed. These are GloSea5 (UKMO System 14; MacLachlan *et al*., 2015), SEAS5 (ECMWF System 5; Johnson *et al*., 2019), and System 7 (Météo-France; http://www.umr-cnrm.fr/IMG/pdf/system7-technical.pdf), and the forecasts contain 62, 51, and 51 ensemble members respectively. Forty member forecasts from the Met Office Decadal Prediction System version 3 (DePreSys3, referred to below as DP3), initialized on first November, are also analysed. DP3 uses the same global coupled model as GloSea5, but is initialized and configured differently, as described in Dunstone *et al*. (2016).

An additional experiment is also run with DP3, in which the top 1,000 m of the Indian Ocean temperature and salinity fields are relaxed towards the negative of the 2019 November IOD anomaly during a five-month spin-up period (June–October). A climatology formed over the previous 5 years (2014–2018) is used to reverse the 2019 anomalies, to avoid the complications of climate change trends. The negative anomaly is simply '2019 values – 2 x climatology' and is applied over the region shown in Figure 2b (smoothly ramped at the boundaries to avoid spatial jumps in temperature or salinity). The atmosphere, however, is nudged identically to the original DP3 ensemble forecast. A freely running 40 member coupled ensemble forecast is then initialised in November using initial conditions from this perturbed-SST integration (exact details of the method are given in Section 5 of Dunstone *et al*., 2019). At this point, the atmosphere can begin to respond to the perturbed Indian Ocean temperatures. The ensemble mean difference of dynamical fields in the original (Orig) DP3 November forecast and this negative IOD (IOD_Neg) forecast allows us to investigate the impacts of the IOD around the globe. These ensembles are referred to below as the 'IOD experiment'. Using a negative IOD anomaly, rather than climatology, doubles the signal size in this ensemble mean difference – important in order to resolve the signal over the noise of internal variability. An implicit assumption here is that the impacts of the IOD on other parts of the globe are linear in the strength of the IOD.

3 | RESULTS

3.1 | The winter 2019/20 NAO and November 2019 IOD

The winter of 2019/20 saw a very strongly positive NAO (1.5 standard deviations above the 1980/81–2019/20 mean; Figure 1a,b). This pattern was well forecast, from November, by the C3S systems and by DP3 (Figure 1c–f). The corresponding higher than average temperatures and greater than average precipitation over the UK and northern Europe were also well forecast by all systems. Due to the signal-to-noise issue (Scaife and Smith, 2018) currently manifest in most seasonal forecasting systems (Baker *et al*., 2018) the ensemble mean signal in all systems is significantly weaker than that seen in the ERA-5 reanalysis.

The forecasts also captured the sub-seasonal evolution between months. A negative anomaly in MSLP was observed over and to the west of the UK in December, transitioning to a positive NAO in January and February. As will be seen below (Figure 3) even this detail was well captured by the seasonal forecast systems. Such a strong level of agreement amongst dynamical forecasting systems on the circulation over the Atlantic and European sector is unusual, and suggests that some common strong forcing from outside of the North Atlantic-European domain drove this MSLP response. Strong tropical forcing is known to exist via teleconnections between ENSO and the NAO, but ENSO was in a neutral state during winter 2019/20.

The IOD, however, was in an extremely positive phase in November 2019 (Lu and Ren, 2020). The DMI, defined in Section 2 and by the green boxes in Figure 2a, attained its second largest positive value since 1972 (red line in Figure 2c shows values back to 1979). In particular, the IOD was exceptionally strong in early winter (Figure 2d compares this winter against all strongly positive IOD years). This positive IOD was captured in forecasts initialised in November 2019 by all the seasonal forecasting systems considered here (not shown).

We therefore investigate the potential impacts of the IOD, beginning by forming composites over extreme positive/negative values of the DMI using the 40 years

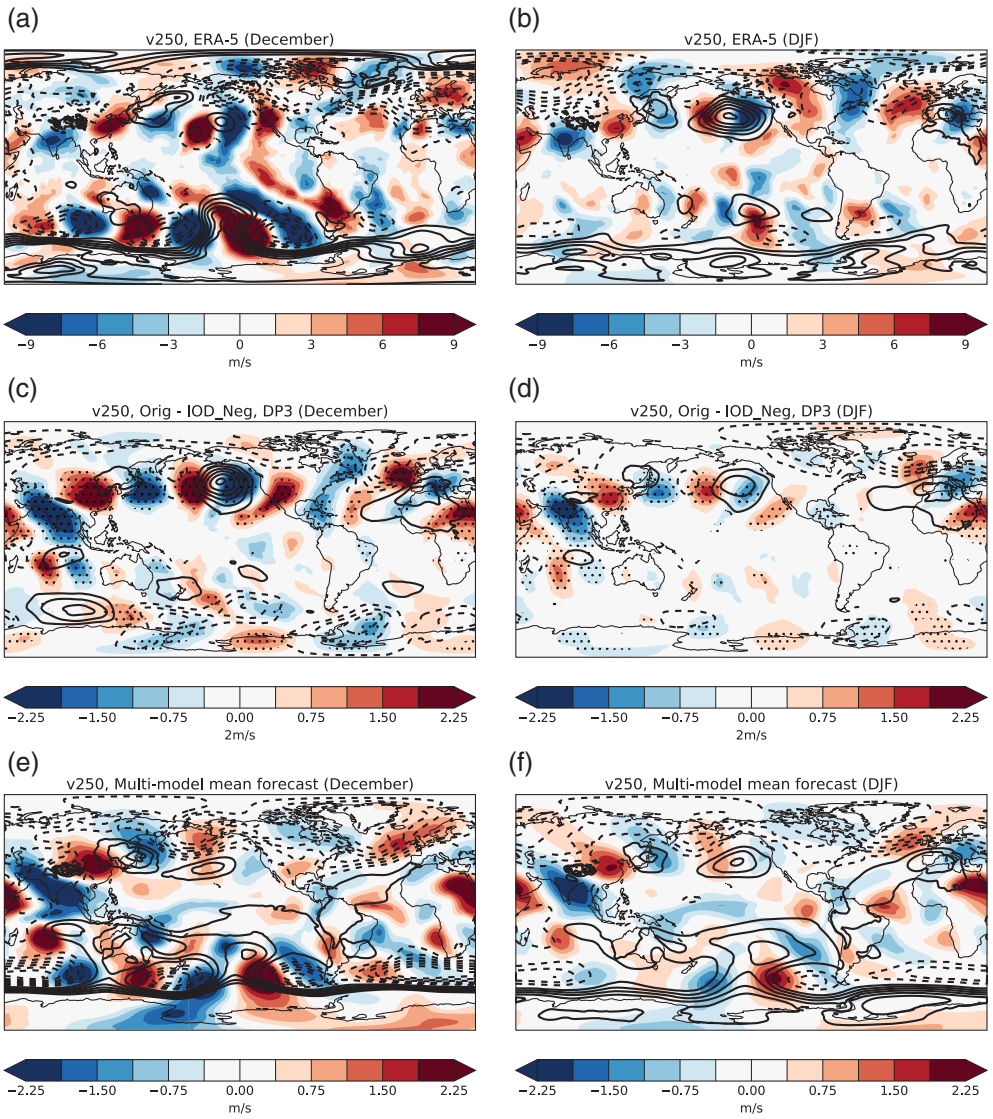

FIGURE 3 Tropospheric pathway. Anomalous v(250 hPa) (m/s) is plotted in coloured shading and anomalous MSLP (hPa) is shown by contours for December 2019 (left panels) and DJF 2019/20 (right panels). (a,b) Observations (ERA-5 anomalies relative to 2014–2018 climatology), (c,d) 'Orig – IOD_Neg' IOD experiment, and (e,f) multi-model ensemble mean forecast using GloSea5, SEAS5, System 7 and DP3. Stippling in (c,d) denotes statistical significance at the 95% level. Positive/negative MSLP contours are shown by solid/dashed lines. The zero MSLP contour is not plotted. MSLP contours (hPa) have the same values as the v250 contours (m/s). The IOD experiment uses double the contour values of the multi-model forecast mean, since the IOD forcing is doubled. The observations use four times the contour values of the multi-model forecast mean (Scaife and Smith, 2018)

1979–2018 from the ERA-5 reanalysis. Since ENSO is known to impact the IOD (Marchant *et al.*, 2007; Liu *et al.*, 2014), the effects of ENSO are removed as far as is possible by using linear regression on the Niño 3.4 index (defined as the area average of SSTs over the region 5°S to 5°N and 190–240°E with the time average removed; Trenberth, 1997). In this way, ENSO effects are removed from both the field over which composites are formed and from the DMI itself (blue line in Figure 2c). MSLP composites on the November DMI show a positive NAO in December–January–February (DJF; Figure 2e). Composites on total precipitation show the corresponding anomalously high rainfall over the UK and northern Europe (Figure 2f) and anomalously low rainfall over southern Europe (Hurrell, 1995), consistent with the winter forecasts and with that experienced in winter 2019/20.

Whilst these composites are highly suggestive that the IOD played a major role in European climate this past winter, composites alone cannot provide evidence of causality (and only the composite on precipitation is statistically significant). However, the 'IOD experiment' described in Section 2 enables us to do this. The ensemble mean difference between the Indian Ocean SSTs in the original (Orig) DP3 November forecast and the negative IOD (IOD_Neg) forecast is shown in Figure 2b, with the green box indicating the region over which the ocean was relaxed prior to the IOD_Neg simulations. Comparing Figure 2b with Figure 2a, and noting the contour levels in Figure 2b are double those in Figure 2a, shows that the desired IOD anomaly has been generated during the November of these ensemble forecasts (panels are not identical since DP3 uses SSTs from Smith and Murphy, 2007, and is an ensemble mean across month 1 of the ensemble integration). In the sections below, the IOD experiment is used to diagnose the impacts of the IOD over the following winter, and thereby investigate the IOD teleconnection pathways.

3.2 | Tropospheric pathway

Rossby wave propagation from the IOD to the Atlantic is diagnosed using anomalous meridional velocity at 250 hPa (v250). Figure 3 shows a wave train originating in the Indian Ocean, and propagating into the Pacific and Atlantic oceans. Since the only difference in the forcing between the 'Orig' and 'IOD_Neg' DP3 simulations is in Indian Ocean temperature and salinity, panels for the IOD experiment (Figure 3c,d) show, by design, only the signal due to changes in the Indian Ocean. These panels show a wave train propagating poleward and eastward from the Indian Ocean, reaching extratropical latitudes across North America, before propagating equatorward again. The wave trains diagnosed from ERA-5 (Figure 3a,b) and the C3S + DP3 multi-model mean forecast (Figure 3e,f) are in very close agreement with the wave train from the IOD experiment, highly suggestive that the Indian Ocean is the key driver of this observed/forecast wave train. As the wave train crosses north America it splits into two paths, one propagating in the mid-latitudes and the other in the high latitudes. This is most clearly seen in December (Figure 3a,c), and is consistent with fig. 7 of Fletcher and Cassou (2015) and with the ENSO tropospheric pathway (shown in fig. 3b,e,h of Jiménez-Esteve and Domeisen (2018)). Once in the Atlantic, the high latitude branch of this wave train projects onto the observed anomalous MSLP pattern (also shown in Figure 3). The DJF mean (Figure 3b,d) is similar, but the wave train for DJF is weaker than that for December. The same conclusions can be drawn from using geopotential height to diagnose the wave trains (Figure S1).

In the winter of 2019/20, the observed anomalous Atlantic MSLP comprises a negative pressure over and to the west of the UK in December, and a positive NAO pattern in DJF (Figure 3a,b). This distinction between December and DJF responses is well captured by the IOD experiment and the C3S multi-model forecasts (compare Figure 3c,e and d,f).

Thus, although it originates in a different location, the IOD tropospheric teleconnection pathway is similar to that for ENSO, consisting of a trans-Pacific-Atlantic wave train, the high latitude branch of which projects onto Atlantic MSLP. The wave train also passes over the location occupied by the climatological Aleutian cyclone in the North Pacific, implications of which will be discussed further in Section 3.3.

3.3 | Stratospheric pathway

As alluded to in the previous section, the stratospheric teleconnection pathway of the IOD to the Atlantic involves the Aleutian cyclone, and is similar to that already documented for ENSO (Manzini *et al.*, 2006; Ineson and Scaife, 2009). Demonstrated best by the IOD

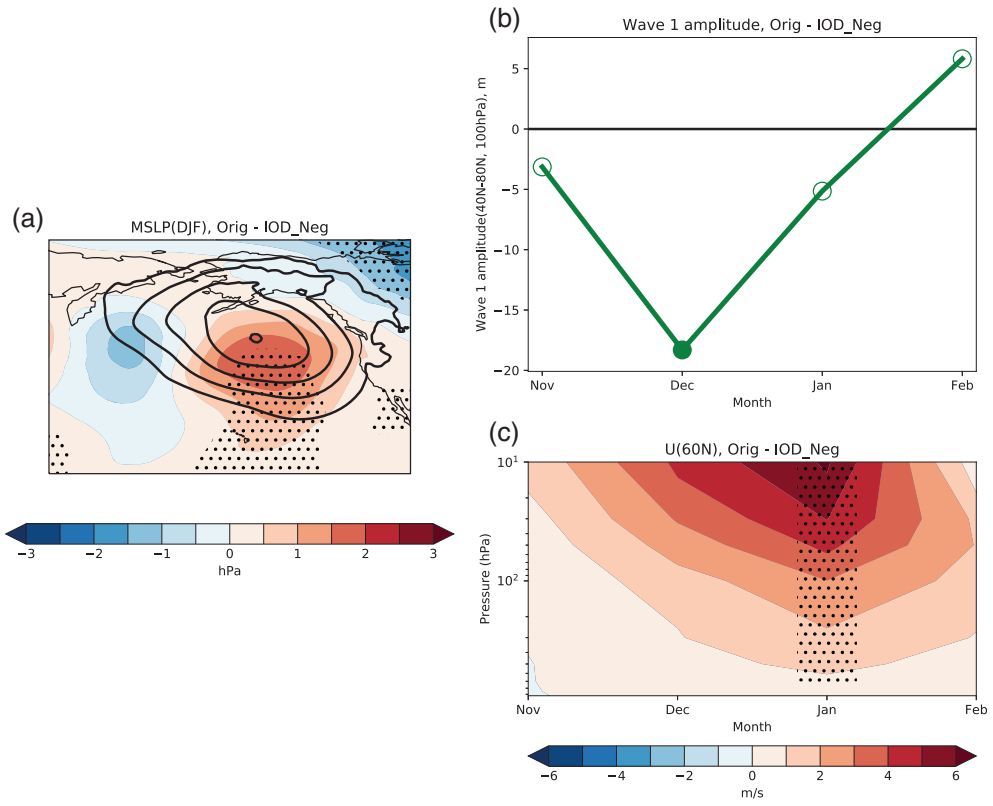

FIGURE 4 Stratospheric pathway. (a) Anomalous MSLP(DJF) for the 'Orig – IOD_Neg' IOD experiment (colours), and anomalous MSLP(DJF) for La Niña–El Niño using HadISST (contours with values 3, 6, 9, 12, and 15 hPa) equivalent to Figure 1 of Ineson and Scaife (2009). (b) Planetary wavenumber 1 amplitude for 'Orig – IOD_Neg' IOD experiment, diagnosed using geopotential height (40–80°N, 100 hPa). Filled circle denotes statistical significance at the 95% level. (c) Anomalous U(60°N) for the 'Orig – IOD_Neg' IOD experiment. Stippling in panels (a) and (c) represents statistical significance at the 95% level

experiment in the month of December, Figure 3c shows a Rossby wave train emerging from the Indian Ocean that leads to poleward flow in the North Pacific near the dateline, and equatorward flow to the east of this. These two responses combine to give anomalously positive MSLP just south of Alaska and the Aleutian Islands. Figure 4a shows that this MSLP anomaly in DJF is in a very similar location to that due to ENSO (shown also in fig. 1 of Ineson and Scaife, 2009). For the single case of winter 2019/20, this signal is evident in early winter, as discussed below, and again in the DJF mean (Figure 3b) due to a particularly strong signal in January and February.

As described in Ineson and Scaife (2009), the positive MSLP anomaly (Figure 4a) acts to reduce the strength of the climatological Aleutian cyclone and, thereby, reduces the amplitude of planetary waves propagating upwards into the stratosphere. Figure 4b demonstrates this reduction in planetary wavenumber 1 amplitude (diagnosed using geopotential height at 100 hPa, area averaged 40–80°N, and then Fourier decomposed; Hardiman *et al*., 2008) in the IOD experiment, and is consistent with fig. 10b of Fletcher and Cassou (2015).

Reduced planetary wave driving in the stratosphere leads to an anomalously strong stratospheric polar vortex (defined by U(60°N, 10 hPa) in Figure 4c, and see also fig. 10 of Fletcher and Cassou, 2015). Anomalously strong vortex signals propagate downwards into the troposphere, resulting in a positive NAO at the surface approximately 1 month later (Baldwin and Dunkerton, 1999; Kidston *et al*., 2015).

In fact, this positive MSLP anomaly in the Aleutian region occurs also in November, so reduced wave driving (Figure 4b) and an anomalously strong stratospheric polar vortex (Figure 4c) are already apparent in

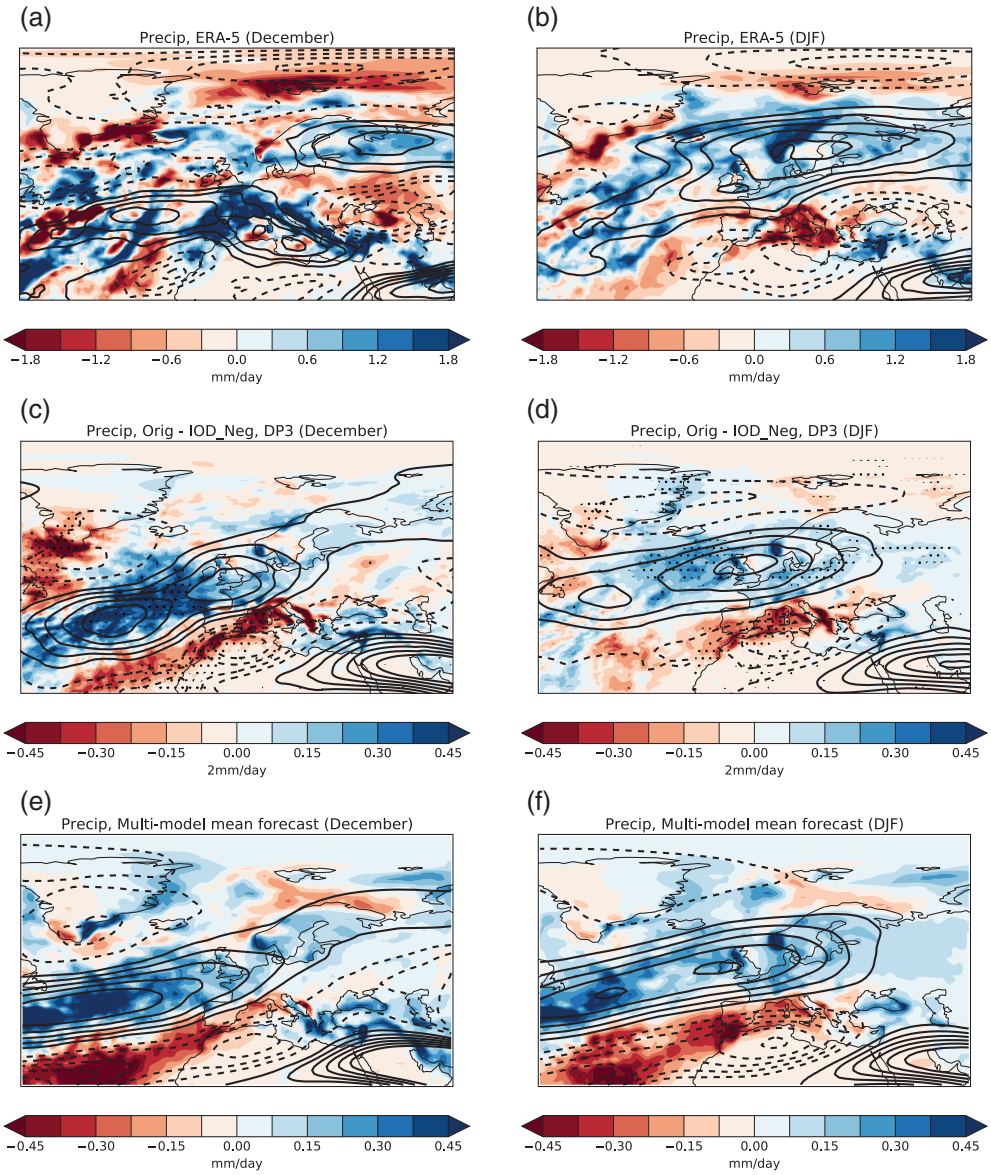

FIGURE 5 Impact on Atlantic jets. As Figure 3, except anomalous total precipitation (mm/day) is plotted in coloured shading, and anomalous u (250 hPa) (m/s) shown by contours. The U contours are in intervals ± (a, b) 2, (c, d) 1, and (e, f) 0.5 m/s, and the zero contour is not plotted

November. Indeed, the November polar vortex strength is anomalously positive in IOD composites, the IOD experiment, ERA-5, and all forecast systems (not shown). Fig. 4 of Nie *et al*. (2019) demonstrated that an early winter preconditioning of the stratospheric polar vortex in November descends through the stratosphere and troposphere in the following winter months, projecting onto an anomalously positive NAO in DJF.

4 | DISCUSSION AND CONCLUSIONS

The winter of 2019/20 was anomalously warm and wet across the UK and Northern Europe, due to a strongly positive NAO. The winter was well forecast by the C3S and the Met Office DP3 seasonal forecast systems. Even the details of individual months, such as the transition from the negative pressure anomaly west of the UK in December to a positive NAO in January/February, were well forecast by all seasonal systems. Such remarkable agreement amongst systems is suggestive of the positive NAO being strongly driven by global influences, and predictable in this case. In this paper, composite analysis and numerical experiments are used to identify the very strong positive IOD event at the start of the winter as the key driver.

Two teleconnection pathways are identified using an experiment in which two ensemble forecasts, one with the observed November 2019 Indian Ocean SST anomalies, and one with the negative of these anomalies, are produced using DP3. The difference in the ensemble mean response, shows a Rossby wave train originating in the Indian Ocean and propagating across the Pacific and Atlantic Oceans. In the Atlantic, this wave train projects directly onto the observed Atlantic MSLP anomalies. In the Pacific, the wave train acts to reduce the amplitude of the Aleutian cyclone and therefore the amplitude of planetary waves propagating into the stratosphere. This results in an anomalously strong stratospheric polar vortex, projecting onto an anomalously positive NAO. This numerical experiment shows good agreement with both the ERA-5 reanalysis data and the C3S multi-model seasonal forecasts in terms of the details of both teleconnection pathways. Furthermore, both pathways are very similar to the well documented tropospheric and stratospheric teleconnection pathways whereby ENSO impacts the north Atlantic MSLP (Hardiman *et al*., 2019).

The impact of the IOD on the Atlantic jet stream and associated precipitation anomalies is a northward shift in the jet latitude, a slight increase in the jet strength, and anomalously high precipitation over the UK and northern Europe, as shown in Figure 5. This is consistent with an anomalously positive NAO and agrees well with the features observed in winter 2019/20. There is a remarkable agreement between the IOD experiment and the C3S multi-model mean forecast. The signal in the December observations is noisier (Figures 3a and 5a), but this is expected, being only a single realisation of a single month.

A knowledge of the teleconnection pathways between the IOD and the North Atlantic gives greater confidence in the seasonal forecast skill they offer. The frequency of positive IOD events has doubled in the 20th century, and their intensity has also increased, with this trend projected to continue (Abram *et al*., 2020). It is likely, therefore, that such connections will become increasingly important for seasonal forecasting of European winters during the rest of the 21st century.

ACKNOWLEDGEMENTS

This work and its contributors (S. C. H., N. J. D., A. A. S., D. M. S., and J. R. K.) were supported by the Met Office Hadley Centre Climate Programme funded by BEIS and Defra. ERA-5 and C3S data were obtained via the Copernicus Climate Data Store. Data and code used to produce all figures and tables can be found at https://doi.org/10.5281/zenodo.3937237.

ORCID

Steven C. Hardiman https://orcid.org/0000-0001-9813-1209
Nick J. Dunstone https://orcid.org/0000-0001-6859-6814
Adam A. Scaife https://orcid.org/0000-0002-5189-7538
Jeff R. Knight https://orcid.org/0000-0003-1868-0852
Richard J. Greatbatch https://orcid.org/0000-0001-5758-2249

REFERENCES

Abram, N.J., Wright, N.M., Ellis, B., Dixon, B.C., Wurtzel, J.B., England, M.H., Ummenhofer, C.C., Philibosian, B., Cahyarini, S.Y., Yu, T.-L., Shen, C.-C., Cheng, H., Edwards, R. L. and Heslop, D. (2020) Coupling of Indo-Pacific climate variability over the last millennium. *Nature*, 579, 385–392. https://doi.org/10.1038/s41586-020-2084-4.

Allan, R. and Ansell, T. (2006) A new globally complete monthly historical gridded mean sea level pressure dataset (HadSLP2): 1850-2004. *Journal of Climate*, 19, 5816–5842. https://doi.org/10.1175/JCLI3937.1.

Bader, J. and Latif, M. (2005) North Atlantic oscillation response to anomalous Indian Ocean SST in a coupled GCM. *Journal of Climate*, 18, 5382–5389. https://doi.org/10.1175/JCLI3577.1.

Baker, H.S., Woollings, T., Forest, C.E. and Allen, M.R. (2019) The linear sensitivity of the North Atlantic oscillation and Eddy-driven jet to SSTs. *Journal of Climate*, 32, 6491–6511. https://doi.org/10.1175/JCLI-D-19-0038.1.

Baker, L.H., Shaffrey, L.C., Sutton, R.T., Weisheimer, A. and Scaife, A.A. (2018) An intercomparison of skill and

overconfidence/underconfidence of the wintertime North Atlantic oscillation in multimodel seasonal forecasts. *Geophysical Research Letters*, 45, 7808–7817. https://doi.org/10.1029/2018GL078838.

Baldwin, M.P. and Dunkerton, T.J. (1999) Propagation of the Arctic oscillation from the stratosphere to the troposphere. *Journal of Geophysical Research*, 104(D24), 30937–30946. https://doi.org/10.1029/1999JD900445.

Cai, W., van Rensch, P., Cowan, T. and Hendon, H.H. (2011) Teleconnection pathways of ENSO and the IOD and the mechanisms for impacts on Australian rainfall. *Journal of Climate*, 24, 3910–3923. https://doi.org/10.1175/2011JCLI4129.1.

Copernicus Climate Change Service (C3S). (2017) *ERA5: Fifth generation of ECMWF atmospheric reanalyses of the global climate*. Copernicus Climate Change Service Climate Data Store (CDS). Available at: https://cds.climate.copernicus.eu/cdsapp#!/home [Accessed 13th April 2020]

Dahlke, S. (2015) *Global Teleconnections Associated with Diabatic Heating Due to Local Rainfall Events*. (Master thesis. Kiel, Germany: Christian-Albrechts-Universität Kiel 71 pp. Available at: http://oceanrep.geomar.de/id/eprint/33768.

Doi, T., Behera, S.K. and Yamagata, T. (2020) Predictability of the super IOD event in 2019 and its link with El Niño Modoki. *Geophysical Research Letters*, 47, e2019GL086713. https://doi.org/10.1029/2019GL086713.

Dunstone, N., Scaife, A.A., MacLachlan, C., Knight, J., Ineson, S., Smith, D., Thornton, H., Gordon, M., McLean, P., Palin, E., Hardiman, S. and Walker, B. (2018) Predictability of European winter 2016/2017. *Atmospheric Science Letters*, 19, e868. https://doi.org/10.1002/asl.868.

Dunstone, N., Smith, D., Hardiman, S., Eade, R., Gordon, M., Hermanson, L., Kay, G. and Scaife, A. (2019) Skilful real-time seasonal forecasts of the dry Northern European summer 2018. *Geophysical Research Letters*, 46, 12368–12376. https://doi.org/10.1029/2019GL084659.

Dunstone, N.J., Smith, D.M., Scaife, A.A., Hermanson, L., Eade, R., Robinson, N., Andrews, M. and Knight, J. (2016) Skilful predictions of the winter North Atlantic oscillation one year ahead. *Nature Geoscience*, 9, 809–814. https://doi.org/10.1038/ngeo2824.

Fletcher, C.G. and Cassou, C. (2015) The dynamical influence of separate teleconnections from the Pacific and Indian Oceans on the northern annular mode. *Journal of Climate*, 28, 7985–8002. https://doi.org/10.1175/JCLI-D-14-00839.1.

Gollan, G. and Greatbatch, R.J. (2017) The relationship between northern hemisphere winter blocking and tropical modes of variability. *Journal of Climate*, 30, 9321–9337. https://doi.org/10.1175/JCLI-D-16-0742.1.

Hardiman, S.C., Dunstone, N.J., Scaife, A.A., Smith, D.M., Ineson, S., Lim, J. and Fereday, D. (2019) The impact of strong El Niño and La Niña events on the North Atlantic. *Geophysical Research Letters*, 46, 2874–2883. https://doi.org/10.1029/2018GL081776.

Hardiman, S.C., Kushner, P.J. and Cohen, J. (2008) Investigating the ability of general circulation models to capture the effects of Eurasian snow cover on winter climate. *Journal of Geophysical Research*, 113, D21123. https://doi.org/10.1029/2008JD010623.

Hoerling, M.P., Hurrell, J.W., Xu, T., Bates, G.T. and Phillips, A.S. (2004) Twentieth century North Atlantic climate change. Part II: Understanding the effect of Indian Ocean warming. *Climate Dynamics*, 23, 391–405. https://doi.org/10.1007/s00382-004-0433-x.

Hurrell, J.W. (1995) Decadal trends in the North Atlantic oscillation: regional temperatures and precipitation. *Science*, 269 (5224), 676–679. https://doi.org/10.1126/science.269.5224.676.

Ineson, S. and Scaife, A.A. (2009) The role of the stratosphere in the European climate response to El Niño. *Nature Geoscience*, 2, 32–36. https://doi.org/10.1038/ngeo381.

Jiménez-Esteve, B. and Domeisen, D.I. (2018) The tropospheric pathway of the ENSO–North Atlantic Teleconnection. *Journal of Climate*, 31, 4563–4584. https://doi.org/10.1175/JCLI-D-17-0716.1.

Johnson, S.J., Stockdale, T.N., Ferranti, L., Balmaseda, M.A., Molteni, F., Magnusson, L., Tietsche, S., Decremer, D., Weisheimer, A., Balsamo, G., Keeley, S.P.E., Mogensen, K., Zuo, H. and Monge-Sanz, B.M. (2019) SEAS5: the new ECMWF seasonal forecast system. *Geoscientific Model Development*, 12, 1087–1117. https://doi.org/10.5194/gmd-12-1087-2019.

Kidston, J., Scaife, A.A., Hardiman, S.C., Mitchell, D.M., Butchart, N., Baldwin, M.P. and Gray, L.J. (2015) Stratospheric influence on tropospheric jet streams, storm tracks and surface weather. *Nature Geoscience*, 8, 433–440. https://doi.org/10.1038/NGEO2424.

Liu, L., Xie, S., Zheng, X., Li, T., Du, Y., Huang, G. and Yu, W. (2014) Indian Ocean variability in the CMIP5 multi-model ensemble: the zonal dipole mode. *Climate Dynamics*, 43, 1715–1730. https://doi.org/10.1007/s00382-013-2000-9.

Liu, N., Chen, H. and Lü, L. (2007) Teleconnection of IOD signal in the upper troposphere over southern high latitudes. *Journal of Oceanography*, 63, 155–157. https://doi.org/10.1007/s10872-007-0014-9.

Lu, B. and Ren, H.-L. (2020) What caused the extreme Indian Ocean dipole event in 2019? *Geophysical Research Letters*, 47, e2020GL087768. https://doi.org/10.1029/2020GL087768.

MacLachlan, C., Arribas, A., Peterson, K.A., Maidens, A., Fereday, D., Scaife, A.A., Gordon, M., Vellinga, M., Williams, A., Comer, R.E., Camp, J., Xavier, P. and Madec, G. (2015) Global seasonal forecast system version 5 (GloSea5): a high-resolution seasonal forecast system. *Quarterly Journal of the Royal Meteorological Society*, 141, 1072–1084. https://doi.org/10.1002/qj.2396.

Manzini, E., Giorgetta, M.A., Esch, M., Kornblueh, L. and Roeckner, E. (2006) The influence of sea surface temperatures on the northern winter stratosphere: ensemble simulations with the MAECHAM5 model. *Journal of Climate*, 19, 3863–3881. https://doi.org/10.1175/JCLI3826.1.

Marchant, R., Mumbi, C., Behera, S. and Yamagata, T. (2007) The Indian Ocean dipole – the unsung driver of climatic variability in East Africa. *African Journal of Ecology*, 45, 4–16. https://doi.org/10.1111/j.1365-2028.2006.00707.x.

Min, J., Zhou, Q., Liu, N., Gao, Q. and Guan, Z. (2008) Teleconnection mode between IOD and northern hemisphere tropospheric circulation and its mechanism. *Meteorology and Atmospheric Physics*, 100, 207–215. https://doi.org/10.1007/s00703-008-0304-9.

Nie, Y., Scaife, A.A., Ren, H.-L., Comer, R.E., Andrews, M.B., Davis, P. and Martin, N. (2019) Stratospheric initial conditions provide seasonal predictability of the North Atlantic and Arctic

oscillations. *Environmental Research Letters*, 14, 034006. https://doi.org/10.1088/1748-9326/ab0385.

Rao, S.A., Behera, S.K., Masumoto, Y. and Yamagata, T. (2002) Interannual subsurface variability in the tropical Indian Ocean with a special emphasis on the Indian Ocean dipole. *Deep Sea Research-II*, 49, 1549–1572. https://doi.org/10.1016/S0967-0645(01)00158-8.

Rayner, N.A., Parker, D.E., Horton, E.B., Folland, C.K., Alexander, L.V., Rowell, D.P., Kent, E.C. and Kaplan, A. (2003) Global analyses of sea surface temperature, sea ice, and night marine air temperature since the late nineteenth century. *Journal of Geophysical Research*, 108(D14), 4407. https://doi.org/10.1029/2002JD002670.

Saji, N., Goswami, B., Vinayachandran, P. and Yamagata, T. (1999) A dipole mode in the tropical Indian Ocean. *Nature*, 401, 360–363. https://doi.org/10.1038/43854.

Saji, N.H. and Yamagata, T. (2003) Possible impacts of Indian Ocean dipole mode events on global climate. *Climate Research*, 25, 151–169. https://doi.org/10.3354/cr025151.

Scaife, A.A., Comer, R., Dunstone, N., Fereday, D., Folland, C., Good, E., Gordon, M., Hermanson, L., Ineson, S., Karpechko, A., Knight, J., MacLachlan, C., Maidens, A., Peterson, K.A., Smith, D., Slingo, J. and Walker, B. (2017b) Predictability of European winter 2015/2016. *Atmospheric Science Letters*, 18, 38–44. https://doi.org/10.1002/asl.721.

Scaife, A.A., Comer, R.E., Dunstone, N.J., Knight, J.R., Smith, D.M., MacLachlan, C., Martin, N., Peterson, K.A., Rowlands, D., Carroll, E.B., Belcher, S. and Slingo, J. (2017a) Tropical rainfall, Rossby waves and regional winter climate predictions. *Quarterly Journal of the Royal Meteorological Society*, 143, 1–11. https://doi.org/10.1002/qj.2910.

Scaife, A.A. and Smith, D. (2018) A signal-to-noise paradox in climate science. *NPJ Climate and Atmospheric Science*, 1, 28. https://doi.org/10.1038/s41612-018-0038-4.

Smith, D.M. and Murphy, J.M. (2007) An objective ocean temperature and salinity analysis using covariances from a global climate model. *Journal of Geophysical Research*, 112, C02022. https://doi.org/10.1029/2005JC003172.

Trenberth, K.E. (1997) The definition of El Niño. *Bulletin of the American Meteorological Society*, 78, 2771–2777. https://doi.org/10.1175/1520-0477(1997)078<2771:TDOENO>2.0.CO;2.

Webster, P., Moore, A., Loschnigg, J. and Leben, R.R. (1999) Coupled ocean–atmosphere dynamics in the Indian Ocean during 1997–98. *Nature*, 401, 356–360. https://doi.org/10.1038/43848.

Weller, E. and Cai, W. (2013) Asymmetry in the IOD and ENSO teleconnection in a CMIP5 model ensemble and its relevance to regional rainfall. *Journal of Climate*, 26, 5139–5149. https://doi.org/10.1175/JCLI-D-12-00789.1.

SUPPORTING INFORMATION

Additional supporting information may be found online in the Supporting Information section at the end of this article.

How to cite this article: Hardiman SC, Dunstone NJ, Scaife AA, *et al.* Predictability of European winter 2019/20: Indian Ocean dipole impacts on the NAO. *Atmos Sci Lett*. 2020;21:e1005. https://doi.org/10.1002/asl.1005